Available online at www.sciencedirect.com

ScienceDirect

Ceramics International 40 (2014) 5061–5066

CERAMICS INTERNATIONAL

www.elsevier.com/locate/ceramint

Short communication

Concentration quenching of Eu^{2+} in $Ba_2LiB_5O_{10}$:Eu^{2+} phosphor

Yufeng Liu[a,*], Yanjun Ding[a], Zhimin Peng[a], Quanmao Yu[b], Xiaodong Tian[c], Guoyi Dong[c]

[a]State Key Lab of Power Systems, Department of Thermal Engineering, Tsinghua University, Beijing 100084, China
[b]Institute of Functional Materials, Jiangxi University of Finance & Economics, Nanchang 330013, PR China
[c]College of Physics Science and Technology, Hebei University, Baoding 071002, PR China

Received 27 June 2013; received in revised form 7 September 2013; accepted 7 September 2013
Available online 16 September 2013

Abstract

An intense orange-reddish-emitting phosphor, Eu^{2+} doped $Ba_2LiB_5O_{10}$ was prepared by solid-state reactions. The excitation spectrum showed a broad band from 250 nm to 400 nm with an intense peak at 322 nm. Under the excitation of 322 nm, the emission band showed one large broad band peaking at about 590 nm with full width at half maximum of 128 nm, which corresponds to the $4f^65d^1 \rightarrow 4f^7$ transition of Eu^{2+}. The critical quenching concentration of Eu^{2+} in $Ba_2LiB_5O_{10}$:Eu^{2+} phosphor was about 3 mol%. The corresponding concentration quenching mechanism was verified to be a dipole–dipole interaction. The value of the critical transfer distance was calculated to be about 19 Å. The CIE coordinate (x, y) did not change from the value (0.54, 0.35) observed for 3 mol% of Eu^{2+} when Eu^{2+} concentration was changed.

Keywords: A. Solid-state reaction; C. Optical properties; Luminescence; Phosphors

1. Introduction

A large number of borate compounds are transparent over a wide spectral range, beginning from ultraviolet (UV) and extending into visible [1,2]. This is one of the reasons that borate compounds become important optoelectronic materials. The alkaline earth orthoborate is known as an efficient phosphor with good stability [3–7]. Saubat first obtained a family of rare earth magnesium borates $LnMgB_5O_{10}$ (Ln=La to Er) in which the Ln^{3+} ions occupy oxygen edge-sharing polyhedra forming isolated chains [8]. Since the crystal structure of $Ba_2LiB_5O_{10}$ was first reported by Huang [9], there are several papers studied the structure and rare earth ions luminescence in this host [10–17]. Dirksen and Blasse investigated the luminescence of Eu^{2+} and Pb^{2+} ions on barium sites in the pentaborate $Ba_2LiB_5O_{10}$ at low temperature of 4.2 K and found both ions show efficient emission with large Stokes shift [12]. Recently, the emission of Eu^{2+} in $Ba_2LiB_5O_{10}$ was reported by many researchers [13,14,16,18]. Su and coworkers synthesized $Ba_2LiB_5O_{10}$:RE^{3+} (RE=Dy, Tb and Tm) using high-temperature solid-state reaction method and studied their thermoluminescence properties under the γ-ray irradiation [15]. In their previous work, it is found that $Ba_2LiB_5O_{10}$ are good host for rare earth ions doped phosphor. However, there is no systematical study of the room temperature photoluminescence properties of Eu^{2+} in $Ba_2LiB_5O_{10}$ including the emission and excitation spectra, the decay time of the emission, concentration quenching and CIE chromaticity coordinates. This is the motivation of our current study of the fluorescence properties of Eu^{2+} ions in this pentaborates.

The structure of $Ba_2LiB_5O_{10}$ contains a one-dimensional polyborate anion built from BO_3 and BO_4 groups. The Li^+ ions are in tetrahedral coordination, the Ba^{2+} ions in an irregular eight coordination. The average Ba^{2+}–O^{2-} distance is relatively long, 2.84 Å vs the expected 2.80 Å. The individual distances range from 2.64 to 3.02 Å, the shorter distances being on one side of the Ba^{2+} ion [10]. Since borates are suitable host lattices for luminescent materials, and with particular interest of the peculiar Ba^{2+} coordination and some peculiar characteristics of Eu^{2+} emission in $Ba_2LiB_5O_{10}$, in this paper, we synthesized $Ba_2LiB_5O_{10}$:Eu^{2+} phosphors and systematically investigated the room temperature photoluminescence properties of Eu^{2+} in $Ba_2LiB_5O_{10}$. Some differences are observed in the Eu^{2+} emission compared to those previously reported by Dirksen and Blasse [12]. Furthermore,

*Corresponding author. Tel.: +86 010 62791873; fax: +86 010 62773005.
E-mail address: liuyufeng4@126.com (Y. Liu).

0272-8842/$ - see front matter © 2013 Elsevier Ltd and Techna Group S.r.l. All rights reserved.
http://dx.doi.org/10.1016/j.ceramint.2013.09.026

in order to further study the interaction between the host lattice and the luminescent properties of the phosphors at room temperature, the relationship of Eu^{2+} luminescence, the Eu^{2+} critical concentration and the mechanism of energy transfer in $Ba_2LiB_5O_{10}:Eu^{2+}$ phosphor is determined in this paper.

2. Experimental

The $Ba_{2-x}LiB_5O_{10}:xEu^{2+}$ $(0.001 \le x \le 0.10)$ phosphors were synthesized by high temperature solid-state reaction method. $BaCO_3$ (99.9%), Li_2CO_3 (99.9%), H_3BO_3 (99.9%) and Eu_2O_3 (99.99%) were used as starting materials. The raw materials with stoichiometrical ratio were weighed and sufficiently mixed in mortar. Excess of H_3BO_3 (about 3 mol%) was added to compensate the evaporation loss at high temperature [19,20]. The impurity phase will appear when less H_3BO_3 was added. On the contrary, more H_3BO_3 will lead to the glass state and low luminescent intensity. In order to obtain the target compound with pure phase, two firing steps were necessary. The mixture was firstly heated at 400 °C for 2 h in a covered alumina crucible, then reground thoroughly after being cooled down to the room temperature. In order to make more Eu^{3+} deoxygenized to Eu^{2+}, the second firing was conducted at 800 °C for 8 h in strong reducing atmosphere (25% H_2/75% N_2). (The very small amount of Eu^{3+} will not affect the emission of Eu^{2+}). The obtained powders were $Ba_2LiB_5O_{10}:Eu^{2+}$ phosphors.

The powder sample was characterized by XRD in a Bruker AXS D8 advanced automatic diffractometer (Bruker Co., German) with Cu $K_{\alpha1}$ radiation (λ=1.5406 Å, 40 kV, 40 mA). Photoluminescence excitation and emissions spectra were measured by using Hitachi F-4600 spectrofluorometer equipped with a 150 W Xenon lamp as an excitation source. This spectrofluorometer was well intensity-calibrated for the excitation and emission spectra. The Commission Internationale de l'Eclairage (CIE) chromaticity coordinates were measured by PMS-80 Plus-UV–Vis-near-IR spectrophoto colorimeter. All of the measurements were conducted at room temperature.

3. Results and discussion

3.1. Crystal structure

Fig. 1 shows the representative XRD patterns of $Ba_2LiB_5O_{10}:Eu^{2+}$ sample containing 3 mol% of Eu^{2+}. For comparison, reference data from Huang et al. is reproduced in Fig. 1 (JCPDS data) [9]. All of the observed diffraction peaks of the $Ba_2LiB_5O_{10}:Eu^{2+}$ sample that was synthesized herein can be basically indexed following the reported data of pure $Ba_2LiB_5O_{10}$ (JCPDS No. 37-0753), with a small shift of diffraction profile toward higher two-theta direction which may be associated with the smaller Eu^{2+} substitutes for larger Ba^{2+} to form the compound. Therefore, our sample shows the same crystal structure as reported in the literature. Huang et al. first synthesized $Ba_2LiB_5O_{10}$ and studied its crystal structure [9,11]. Smith and Keszler gave the details of the same structure

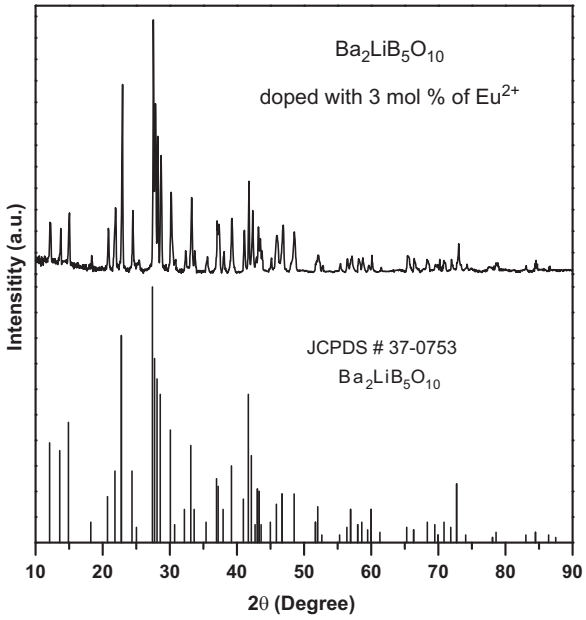

Fig. 1. XRD pattern of typical sample $Ba_2LiB_5O_{10}$ doped with 3 mol% of Eu^{2+} annealed at 800 °C and the standard data JCPDS card No. 37-0753 of $Ba_2LiB_5O_{10}$ as reference.

[10]. $Ba_2LiB_5O_{10}$ has a monoclinic unit cell with space group *Pmma* (51) and lattice parameters a=4.413 Å, b=14.585 Å, c=6.700 Å, and V_{cell}=417.9 Å^3.

Fig. 2 shows the sketch of the $Ba_2LiB_5O_{10}$ crystal structure. The structure is composed of Li and Ba cations and $[B_5O_{10}]^{5-}$ anions. $[B_5O_{10}]^{5-}$ is a moiety composed of three triangular BO_3 units and two tetrahedral BO_4 units [10,11]. From the crystal structure, there is only one type of Ba sites, which has distinct effect on the optical properties of Eu^{2+}-doped $Ba_2LiB_5O_{10}$. This will be discussed subsequently in connection with the luminescence properties of $Ba_2LiB_5O_{10}:Eu^{2+}$. It is known that the ionic radii (r) of Ba^{2+} (CN=8) and Li^+ (CN=4) are 1.42 Å and 0.59 Å, respectively. The ionic radius of B^{3+} is 0.01 Å when CN=3 and 0.11 Å when CN=4 [21]. As a result of the ionic radii of doping Eu^{2+} (CN=8, r=1.25 Å), it is difficult for Eu^{2+} to substitute Li^+ or B^{3+} in the $Ba_2LiB_5O_{10}$. Hence, in this study, based on the structure analysis above, it is believed that the Ba^{2+} sites are replaced by Eu^{2+} in the lattice because they have the same valence state and very similar ionic radii.

3.2. Photoluminescence of $Ba_2LiB_5O_{10}:Eu^{2+}$

The energetic position of the Eu^{2+} emission is highly sensitive to the crystal field environments. The $4f^65d \rightarrow 4f^7(^8S_{7/2})$ transition of Eu^{2+} occurs from the lowest levels of $4f^65d$ excited electronic state. The emission and excitation spectra of the sample $Ba_2LiB_5O_{10}:Eu^{2+}$ doped with 3 mol% of Eu^{2+} phosphors are presented in Fig. 3. Excited by the excitation wavelength of 322 nm, the phosphor exhibits an orange reddish emission and shows one large broad band peaking at about 590 nm with full width at half maximum of about 128 nm. This corresponds to the f–d transition of Eu^{2+}. There

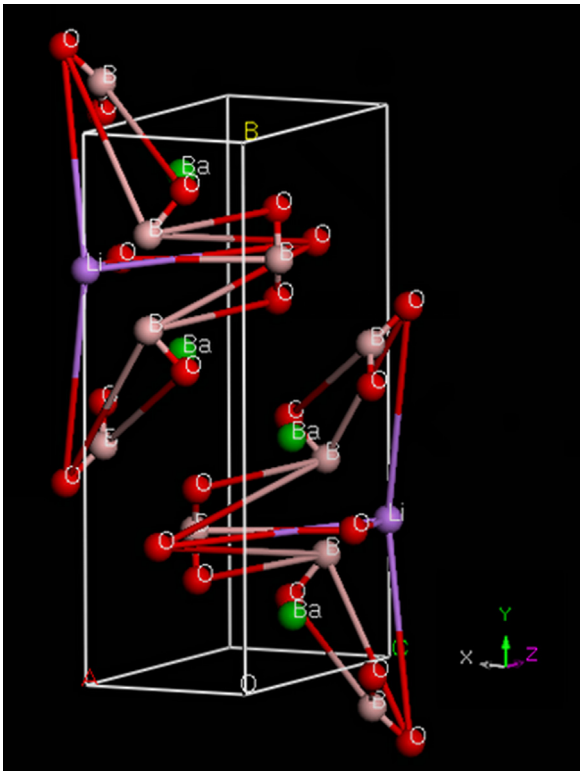

Fig. 2. The sketch of the $Ba_2LiB_5O_{10}$ crystal structure.

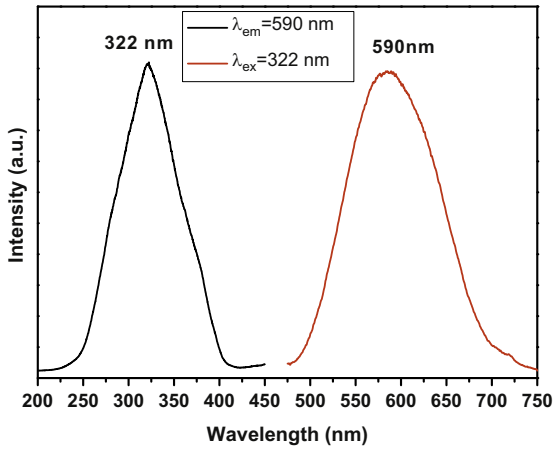

Fig. 3. The emission and excitation spectra of typical sample phosphors $Ba_2LiB_5O_{10}$ doped with 3 mol% of Eu^{2+}.

is an overlap of the 5*d* energy level of Eu^{2+} and the lower level of 4*f* state, so the electrons of the 4*f* state can be excited to the 5*d* state. The broad luminescence of Eu^{2+} is due to the $4f^6 5d^1 \rightarrow 4f^7$ transition, which is an allowed electrostatic dipole transition. However, the 5*d* state is easily affected by the crystal field; therefore, different crystal fields can split the 5*d* state in different ways [22]. In $Ba_2LiB_5O_{10}$ crystal structure, the Ba atom occupies an eight-coordinate site with Ba-O distances ranging from 2.64 to 3.02 Å. The codopant Eu^{2+} ions are substituted for the Ba^{2+} sites and are exposed to a strong crystal field, the excitation band of Eu^{2+} shows broad band from 250 nm to 400 nm with one intense peak located at

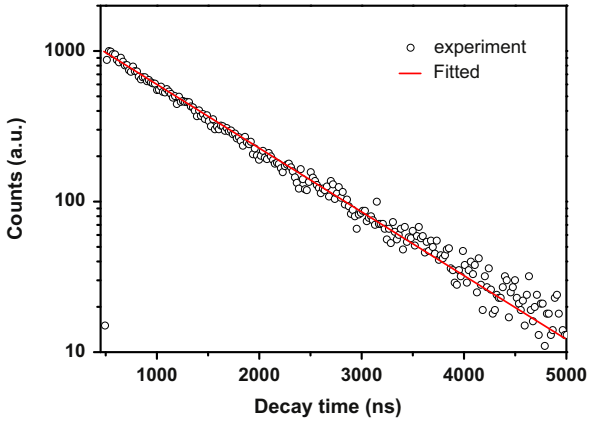

Fig. 4. The decay time of 590 nm emission for the typical sample phosphors $Ba_2LiB_5O_{10}:Eu^{2+}$ doped with 3 mol% of Eu^{2+}.

322 nm. A rough estimate of the Stokes shift can be calculated from the excitation band (322 nm) and the corresponding emission band (590 nm). In this way, the Stokes shift of $Ba_2LiB_5O_{10}:Eu^{2+}$ is estimated to be approximately 268 nm according to the luminescence spectra in Fig. 3, and the calculated Stokes shift is similar to that observed by Dirksen and Blasse for $Ba_2LiB_5O_{10}:Eu^{2+}$ [12].

Fig. 4 shows fluorescence decay curves of 590 nm emissions for $Ba_2LiB_5O_{10}:Eu^{2+}$ doped with 3 mol% of Eu^{2+}. It is well-known that the decay behavior can be represented as

$$I = I_0 \exp(-t/\tau) \quad (1)$$

where I and I_0 are the luminescence intensities at time t and 0, respectively, and τ is the luminescence lifetime. The lifetimes of the Eu^{2+} emissions in $Ba_2LiB_5O_{10}:Eu^{2+}$ were calculated to be about 0.95 μs for the 590 nm emissions by using this equation. The result is in agreement with the report of Poort [23].

3.3. Critical transfer distance (R_c) in $Ba_2LiB_5O_{10}:Eu^{2+}$ phosphor

To study the concentration quenching process of Eu^{2+} ions in $Ba_2LiB_5O_{10}:Eu^{2+}$ phosphors, the excitation and emission spectra of phosphors with different Eu^{2+} content (0.1 mol%, 1 mol%, 3 mol%, 5 mol%, 7 mol% and 10 mol%) excited by 322 nm are investigated. There is no obvious change in the positions of excitation and emission bands for all the samples as shown in Fig. 5. It can be seen that as Eu^{2+} concentration increases, the emission intensity increases and reaches the maximum at 3 mol%. Concentration quenching occurs, when the Eu^{2+} concentration is more than 3 mol%.

While considering the mechanism of energy transfer in oxide phosphors, Blasse pointed out that if the activator is introduced solely on *Z* ion sits, x_c is the critical concentration, *N* is the number of *Z* ions in the unit cell and *V* is the volume of the unit cell, then there is on the average of one activator ion per V/x_cN. The critical transfer distance (R_c) is approximately

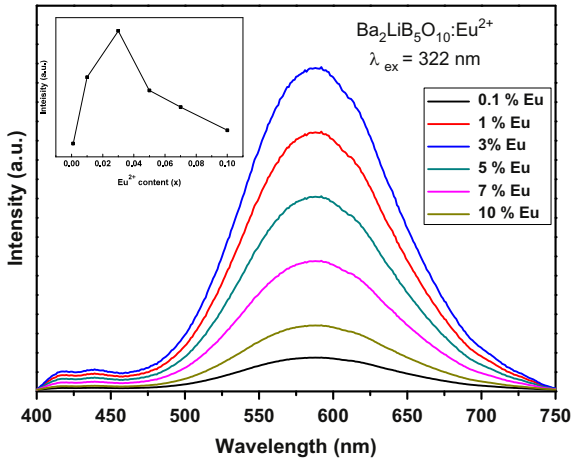

Fig. 5. The Eu^{2+} emission intensities at 590 nm as a function of Eu^{2+} concentration.

equal to twice the radius of a sphere with the volume [24]

$$R_c \approx 2\left[\frac{3V}{4\pi x_c N}\right]^{1/3} \quad (2)$$

By taking the appropriate values of V, N and x_c (417.9 Å^3, 4, 0.03, respectively), the critical transfer distance of Eu^{2+} in $Ba_2LiB_5O_{10}$:Eu^{2+} phosphor is found to be 18.8 Å. According to Dexter's theory on non-radiative energy transfer, the critical transfer of Eu^{2+} can also be calculated from the spectral experimental data. The value of the critical transfer distance (R_c) can be found from [25]

$$R_c^6 = 0.63 \times 10^{28}\frac{4.8 \times 10^{-16}P}{E^4}S.O. \quad (3)$$

where P is the oscillator strength of the absorption transition of the Eu^{2+} ion, E the energy of maximum spectral overlap, and $S.O.$ the spectral overlap integral. For P a value of 10^{-2} for the broad $4f^7 \rightarrow 4f^6 5d^1$ absorption band is taken [24]. E and $S.O.$, which are derived from the spectral experimental data, are 2.8 eV and 0.1 eV^{-1}. According to these data, a value of $R_c = 19.1$ Å is obtained. Thus, the R_c value based on the calculated crystal structure data is in good agreement with that of the experimental spectral data.

3.4. Mechanism of energy transfer in $Ba_2LiB_5O_{10}$:Eu^{2+} phosphor

Non-radiative energy transfer from a Eu^{2+} ion to another Eu^{2+} ion may occur by exchange interaction, radiation reabsorption or multiple–multiple interaction, Eu^{2+} is an isolated emission center in $Ba_2LiB_5O_{10}$:Eu^{2+} phosphors. The $4f^7 \rightarrow 4f^6 5d^1$ transition of Eu^{2+} is allowed while exchange interaction is responsible for the energy for forbidden transitions and typical critical distances are then about 5 Å [25]. This indicates that the mechanism of exchange interaction does not play a significant role in energy transfer between Eu^{2+} ions in $Ba_2LiB_5O_{10}$:Eu^{2+} phosphor. The mechanism of radiation reabsorption becomes important when there is broad overlap of the fluorescent spectra of the sensitizer and activator which is not the case by examining the emission and excitation spectra of $Ba_2LiB_5O_{10}$:Eu^{2+} phosphor. According to Dexter's theory, the energy transfer mechanism of Eu^{2+} emission in $Ba_2LiB_5O_{10}$:Eu^{2+} phosphor is attributed to the electric multiple–multiple interaction [25].

When the electric multipolar interaction is involved in the energy transfer, there are several types of interactions [such as dipole–dipole (d–d), dipole–quadrupole (d–q), quadrupole–quadrupole (q–q) interactions, and so on]. It is necessary to elucidate which type of interaction is involved in the energy transfer. According to Vanuitert's study that if the energy transfer occurs among the same sorts of activators, the strength of the multipolar interaction can be determined from the change of the emission intensity level which has the multipolar interaction. The emission intensity (I) per activator ion follows the equation [26]:

$$I/x = k[1+\beta(x)^{\theta/3}]^{-1} \quad (4)$$

where x is the activator concentration, I/x is the emission intensity (I) per activator (x). K and β are constants for a given host under the same excitation condition. According to Eq. (4), $\theta = 3$ for the energy transfer among the nearest-neighbor ions (exchange interaction), while $\theta = 6$, 8, and 10 for d–d, d–q, and q–q interactions, respectively[26]. Assuming that $\beta(x)^{\theta/3} \gg 1$, Eq. (4) can be simplified as follow [27]:

$$\log I/x = K' - \theta/3 \log x \quad (K' = \log K - \log \beta) \quad (5)$$

From the slope of Eq. (5), the electric multipolar character (θ) can be obtained by the slope ($-\theta/3$) of the plot logI/x vs log$x$. The critical concentration of Eu^{2+} has been determined to be 3 mol%. The dependence of the emission intensity of $Ba_2LiB_5O_{10}$:xEu^{2+} phosphor excited at 322 nm as a function of the corresponding concentration of Eu^{2+} for concentration greater than the critical concentration ($x \geq 0.03$) is determined. The plot of lgI/x as a function of lg$x$ in $Ba_2LiB_5O_{10}$:Eu^{2+} phosphors are shown in Fig. 6. It can be seen that the dependence of lgI/x on lg$x$ of Eu^{2+} is linear and its slope is about -1.96. The value of θ can be calculated as 5.88, which are approximately 6. This indicates that the d–d interaction is

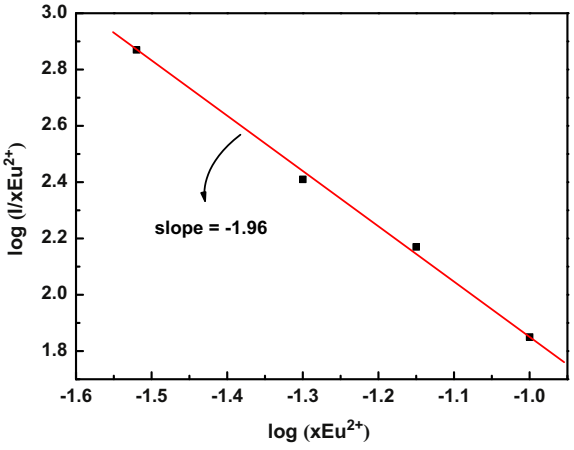

Fig. 6. Log plot for the emission intensity at 608 nm per activator ions (Eu^{2+}) as a function of the activator concentration.

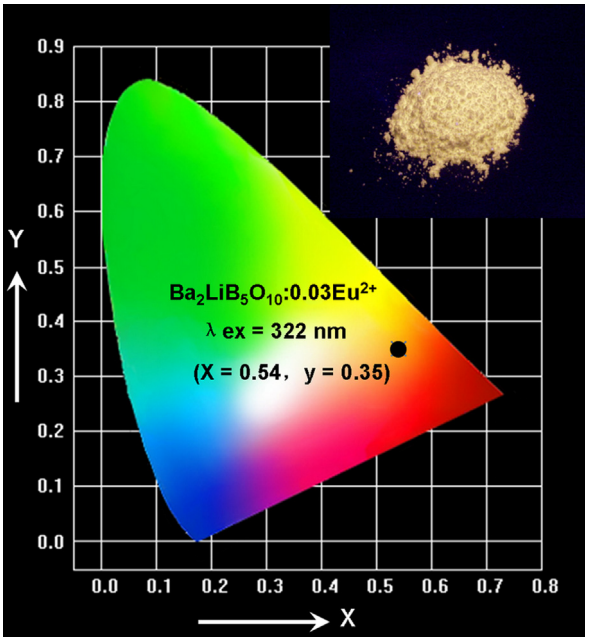

Fig. 7. The CIE chromaticity coordinates for of typical sample $Ba_2LiB_5O_{10}$:Eu^{2+} doped with 3 mol% of Eu^{2+} under the excitation of 322 nm.

the main concentration quenching mechanism of Eu^{2+} emission in the $Ba_2LiB_5O_{10}$:Eu^{2+} phosphor.

3.5. CIE chromaticity coordinates analysis

Color coordinates are one of the important factors for evaluating phosphors' performance. It is a well known fact that the color coordinates are same if the spectra profiles are identical. In such case, the CIE chromaticity coordinates for $Ba_2LiB_5O_{10}$:Eu^{2+} with varying Eu^{2+} concentrations under the excitation of 322 nm are investigated. The chromaticity data were taken based on the intensity-calibrated emission spectra data by using the PMS-80 spectra analysis system. The CIE coordinates of all the samples are $x=0.54$, $y=0.35$, and they are not change with the increasing of Eu^{2+} concentration. Fig. 7 shows the CIE chromaticity coordinate for the typical as-prepared samples $Ba_2LiB_5O_{10}$:$0.03Eu^{2+}$ with the dot symbols ($\lambda_{ex}=322$ nm).

4. Conclusions

In summary, orange reddish emitting phosphors powders $Ba_2LiB_5O_{10}$:Eu^{2+} have been synthesized by solid-state reactions. Eu^{2+} occupied Ba^{2+} sites and form one emission center at about 590 nm. With an increase in the Eu^{2+} concentration, quenching of the excitation energy occurs. The critical quenching concentration of Eu^{2+} in $Ba_2LiB_5O_{10}$:Eu^{2+} phosphor is determined as 3 mol%. The critical transfer distance is calculated as about 19 Å, and it is confirmed by Dexter's theory on energy transfer. The mechanism of concentration quenching of Eu^{2+} in $Ba_2LiB_5O_{10}$:Eu^{2+} phosphor is determined to be d–d interaction. The spectra and chromaticity data indicate that this orange reddish emitting phosphor might be useful for the development of solid state light.

Acknowledgments

This work was financially supported by the National Natural Science Foundation of China (Grant No. 50672020), the Science and Technology Project of Hebei Province (Grant No. E2008000628), the Education Department Fundation of Hebei Province (2009-24-03) and College of Physics Science and the Industry Academy Research Foundation of Hebei University (K201201).

References

[1] B.P. Becker, Borate materials in nonlinear optics, Advanced Materials 10 (1998) 979–992.
[2] H.A. Höppe, Recent developments in the field of inorganic phosphors, Angewandte Chemie International Edition 48 (2009) 3572–3582.
[3] A. Diaz, D.A. Keszler, Red, green, and blue Eu^{2+} luminescence in solid-state borates: a structure-property relationship, Materials Research Bulletin 31 (1996) 147–151.
[4] S.L. Yuan, Y.X. Yang, X.H. Zhang, F. Tessier, F. Cheviré, J.J. Adam, B. Moine, G.R. Chen, Eu^{2+} and Mn^{2+} codoped $Ba_2Mg(BO_3)_2$-a new red phosphor for white LEDs, Optics Letters 33 (2008) 2865–2867.
[5] J.W. Hair, J.T.C. Vankemenade, Third International Conference Science and technology of Light Sources. Toulouse, (1983), p.54.
[6] M. Leskela, M. Saakes, G. Blasse, Energy transfer phenomena in $GdMgB_5O_{10}$, Materials Research Bulletin 19 (1984) 151–159.
[7] B. Saubat, C. Fouassier, P. Hagenmuller, J.C. Bourcet, Luminescent efficiency of Eu^{3+} and Tb^{3+} in $LaMgB_5O_{10}$ type borates under excitation from 100 to 400 nm, Materials Research Bulletin 16 (1981) 193–198.
[8] B. Saubat, M. Vlasse, C. Fouassier, Synthesis and structural study of the new rare earth magnesium borates $LnMgB_5O_{10}$ (Ln=La, Er), Journal of Solid State Chemistry 34 (1980) 271–277.
[9] Q.Z. Huang, G.F. Wang, J.K. Liang, Phase equilibrium relation of BaB_2O_4-$Li_2B_2O_4$ and BaB_2O_4-Li_2O sections in the ternary system BaO-Li_2O-B_2O_3, Acta Physica Sinica 33 (1984) 76–85.
[10] R.W. Smith, D.A. Keszler, The pentaborate $LiBa_2B_5O_{10}$, Materials Research Bulletin 24 (1989) 725–731.
[11] Q.Z. Huang, S.F. Lu, G.Q. Dai, J.K. Liang, A new type of borate double salt: structure of $LiBa_2B_5O_{10}$, Acta Crystallographica C48 (1992) 1576–1578.
[12] G.J. Dirksen, G. Blasse, Luminescence in the Pentaborate $LiBa_2B_5O_{10}$, Journal of Solid State Chemistry 92 (1991) 591–593.
[13] P. Dorenbos, Anomalous luminescence of Eu^{2+} and Yb^{2+} in inorganic compounds, Journal of Physics: Condensed Matter 15 (2003) 2645–2665.
[14] S. Pan, J.P. Smit, C.H. Lanier, M.R. Marvel, L.D. Marks, K. R. Poeppelmeier, Optical floating zone growth of a-BaB_2O_4 from a $LiBa_2B_5O_{10}$-based solvent, Crystal Growth and Design 7 (8) (2007) 1561–1564.
[15] L.Y. Liu, Y.L. Zhang, J.Q. Hao, C.Y. Li, S.B. Wang, Q. Su, Thermoluminescence studies of $LiBa_2B_5O_{10}$:RE^{3+} (RE=Dy, Tb and Tm), Journal of Physics and Chemistry of Solids 68 (2007) 1745–1748.
[16] Q. Wang, D.G. Deng, S.Q. Xu, Y.J. Hua, L.H. Huang, H.P. Wang, S. L. Zhao, Guohua Jia, C.X. Li, Crystal structure and photoluminescence properties of Eu^{2+}-activated $Ba_2LiB_5O_{10}$ phosphors, Optics Communications 284 (2011) 5315–5318.
[17] Y.F. Liu, Z.P. Yang, Q.M. Yu, X. Li, Y.M. Yang, P.L. Li, Luminescence properties of $Ba_2LiB_5O_{10}$:Dy^{3+} phosphor, Materials Letters 65 (2011) 1956–1958.
[18] A. Diaz, D.A Keszler., Eu^{2+} luminescence in the borates $X_2Z(BO_3)_2$ (X=Ba, Sr; Z=Mg, Ca), Chemistry of Materials 9 (1997) 2071–2077.

[19] L.L. Wang, Y.H. Wang, The photoluminescence properties of $CaYBO_4$:Eu^{3+} under UV and VUV region, Journal of Alloys and Compounds 422 (2006) 305–307.

[20] J. Li, J.Q. Hao, C.X. Zhang, Q. Tang, Y.L. Zhang, Q. Su, S.B. Wang, Thermoluminescence characteristics of BaB_4O_7:Dy phosphor, Nuclear Instruments and Methods in Physics Research Section B 222 (2004) 577–582.

[21] R.D. Shannon, Revised effective ionic radii and systematic studies of interatomic distances in halides and chalcogenides, Acta Crystallographica A32 (1976) 751–767.

[22] S.S. Yao, L.H. Xue, Y.W. Yan, Concentration quenching of Eu^{2+} in $Ba_2Mg(BO_3)_2$:Eu^{2+} phosphor, Current Applied Physics 11 (3) (2011) 639–642.

[23] S.H.M. Poort, A. Meyerink, G. Blasse, Lifetime measurements in Eu^{2+}-doped host lattices, Journal of Physics and Chemistry of Solids 58 (9) (1997) 1451–1456.

[24] G. Blasse, Energy transfer between inequivalent Eu^{2+} ions, Journal of Solid State Chemistry 62 (1986) 207–211.

[25] D.L. Dexter, A theory of sensitized luminescence in solids, Journal of Chemical Physics 21 (1953) 836–850.

[26] L.G. Vanuitert, Characterization of energy transfer interactions between rare earth ions, Journal of the Electrochemical Society 114 (1967) 1048–1053.

[27] H.Y. Du, J.F. Sun, Z.G. Xia, J.Y. Sun, Luminescence properties of $Ba_2Mg(BO_3)_2$:Eu^{2+} red phosphors synthesized by a microwave-assisted sol-gel route, Journal of the Electrochemical Society 156 (12) (2009) J361–J366.